

Supporting Information for
**Rare-Earth Oxychalcogenide $\text{Eu}_2\text{ZnGe}_2\text{OS}_6$: A Phase-Matching
Infrared Nonlinear Optical Material with $[\text{GeOS}_3]$ units**

Guili Wang,^{a,b} Wentian Wu,^{a,b} Chunxiao Li,^a and Jiyong Yao^{a,b,*}

a Beijing Center for Crystal Research and Development, Key Lab of Functional Crystals and Laser Technology,

Technical Institute of Physics and Chemistry, Chinese Academy of Sciences, Beijing 100190, P. R. China.

b Center of Materials Science and Optoelectronics Engineering, University of Chinese Academy of Sciences, Beijing

100049, P. R. China.

*Corresponding author:

Jiyong Yao; jyao@mail.ipc.ac.cn.

Table of Contents

Experimental Procedures

1. Reagents
2. Synthesis
3. Elemental analysis
4. Single crystal structure determination
5. Powder X-ray diffraction
6. Optical Characterizations
7. Powder SHG Test
8. Theoretical Calculation

Table S1. Crystallographic data and structure refinement for $\text{Eu}_2\text{ZnGe}_2\text{OS}_6$.

Table S2. Wyckoff site, fractional atomic coordinates ($\times 10^4$), equivalent isotropic displacement parameters U_{eq} ($\text{\AA}^2 \times 10^3$), and BVS for $\text{Eu}_2\text{ZnGe}_2\text{OS}_6$.

Table S3. Selected bond lengths (\AA) and bond angles ($^\circ$) for $\text{Eu}_2\text{ZnGe}_2\text{OS}_6$.

Table S4. The dipole moment direction and magnitude (in Debye) of $[\text{ZnS}_4]^{6-}$ and $[\text{GeOS}_3]^{4-}$ units in $\text{Eu}_2\text{ZnGe}_2\text{OS}_6$.

Figure S1. The element distribution images and atomic percentage (%) of $\text{Eu}_2\text{ZnGe}_2\text{OS}_6$.

Figure S2. The coordination geometry of $\text{Eu}_2\text{ZnGe}_2\text{OS}_6$.

Figure S3. The IR spectrum of $\text{Eu}_2\text{ZnGe}_2\text{OS}_6$.

Figure S4. The Raman spectrum of $\text{Eu}_2\text{ZnGe}_2\text{OS}_6$ (inset: $\text{Eu}_2\text{ZnGe}_2\text{OS}_6$ single crystals).

References

Experimental Procedures

1. Reagents All starting materials, Eu(99.95%), Eu_2O_3 (99.9%), ZnO (99.9%), ZnS (99.9%), Ge (99.999%), S (99.999%), and CsI (99.9%) were directly purchased from Aladdin Co., Ltd. without further purification. The binary compounds EuS and GeS_2 were synthesized by heating the stoichiometric ratios of raw elements in flame-sealed silica tubes at high temperatures. All manipulations were carried out in an argon-filled glovebox.

2. Synthesis For single crystal growth, The mixture of Eu_2O_3 , ZnS , and GeS_2 (molar ratio:1:1:2, total mass 0.3 g) was homogeneously mixed and finely ground with the same mass of CsI and loaded into silica tubes, then these tubes were flame-sealed under a high vacuum of 10^{-3} Pa and placed into a programmable furnace. These tubes were gradually heated to 1223 K from room temperature (RT) in 20 h and kept at 1223 K for 48 h, then slowly cooled to 623 K at a rate of 3 K/h, finally, the furnace was switched off and naturally cooled to RT. In the end, we obtained orange-colored block crystals of $\text{Eu}_2\text{ZnGe}_2\text{OS}_6$. For polycrystalline powder synthesis, the mixture of EuS, ZnO , and GeS_2 at a stoichiometric molar ratio of 2:1:2 was ground and placed into a silica tube. This tube was heated to 1173 K at a rate of 1 K/h and kept for 72 h, then cooled to RT by switching off the furnace.

3. Elemental analysis. Elemental analysis of the single crystal was carried out using a field-emission Hitachi S-4800 scanning electron microscope (SEM) equipped with an OXFORD X-Max^N 80 energy dispersive X-ray spectroscopy (EDS).

4. Single crystal structure Determination. A suitable single crystal of $\text{Eu}_2\text{ZnGe}_2\text{OS}_6$ was selected under an optical microscope for structure determination. Its X-ray diffraction data were collected at 296.15 K employing a Bruker D8 Quest diffractometer (Mo-K_α radiation, $\lambda = 0.71073$ Å) equipped with a CCD area detector. The structure was solved with the SHELXT structure solution program using intrinsic phasing and refined with the SHELXL refinement package using least squares minimisation.¹

5. Powder X-ray Diffraction (PXRD). The polycrystalline powder of $\text{Eu}_2\text{ZnGe}_2\text{OS}_6$ was reground with an agate mortar for PXRD data collection using a Bruker D8 Advance diffractometer equipped with Cu-K_α ($\lambda = 1.5418$ Å) radiation. The collection range is from 10° to 70° with a scan speed of 0.1 s and a scan step width of 0.02° . The simulated pattern was

generated by Mercury software.²

6. Optical Characterizations. The IR spectrum of $\text{Eu}_2\text{ZnGe}_2\text{OS}_6$ was measured using a Varian Excalibur 3100 spectrometer in the range of $400\text{--}4000\text{ cm}^{-1}$. To produce the test samples, dry KBr was completely mixed with $\text{Eu}_2\text{ZnGe}_2\text{OS}_6$ at a mass ratio of about 100 : 1. The UV–vis–NIR diffuse reflectance spectrum was measured in the wavelength range of $200\text{--}2500\text{ nm}$ by an Agilent Carry 7000 spectrophotometer equipped with an integrating sphere at RT, and a polytetrafluoroethylene sample as standard material. The absorption values were calculated from the reflectance data via the Kubelka-Munk function.³ The Raman spectrum of $\text{Eu}_2\text{ZnGe}_2\text{OS}_6$ was measured by a Lab RAM Aramis spectrometer equipped with a 532 nm laser in the range of $100\text{--}500\text{ cm}^{-1}$ at RT.

7. Powder SHG Test. Since $\text{Eu}_2\text{ZnGe}_2\text{OS}_6$ belongs to the non-centrosymmetric (NCS) space group, its SHG intensity was evaluated through the Kurtz-Perry method employing a 2090 nm fundamental laser. The $\text{Eu}_2\text{ZnGe}_2\text{OS}_6$ polycrystalline powder was ground and filtered into samples with four particle sizes ($20\text{--}50$, $50\text{--}90$, $90\text{--}125$, and $125\text{--}150\text{ }\mu\text{m}$). AGS crystals were also ground into the same range and served as the benchmark for the measurements.

8. Theoretical Calculation. Based on density functional theory (DFT), the CASTEP package was used to calculate the properties of $\text{Eu}_2\text{ZnGe}_2\text{OS}_6$ at the atomic level.⁴ The fine calculation quality was adopted. The CA-PZ function under the local density approximation (LDA) was selected as the exchange-correlation functional.⁵ The interactions between valence electrons and ions were described using ultrasoft pseudopotentials (USP) by treating Eu $4f^7 5s^2 5p^6 6s^2$, Zn $3d^{10} 4s^2$, Ge $4s^2 4p^2$, O $2s^2 2p^4$, and S $3s^2 3p^4$ electrons as valence electrons, respectively.⁶ The L(S)DA+U method was used to treat the strongly correlated $4f$ electrons. A dense Monkhorst-Pack k-point grid of $2 \times 2 \times 2$ in the Brillouin zone was chosen for the $\text{Eu}_2\text{ZnGe}_2\text{OS}_6$. The plane-wave cutoff energy in the calculations was set to 830 eV . The properties of the title compound were calculated after geometric optimization to bring the model to the convergence criterion. 0.39 eV (the difference between the experimental and computed band gap) was set as the scissor operator in the computation of optical properties employing the scissors-corrected-LDA method.⁷

Table S1. Crystallographic data and structure refinement for Eu₂ZnGe₂OS₆.

CCDC number	2390087
Empirical formula	Eu ₂ ZnGe ₂ OS ₆
Formula Weight	722.83
Crystal System	Tetragonal
Space Group	$P\bar{4}2_1m$ (113)
T/K	296.15
a (Å)	9.3838(7)
b (Å)	9.3838(7)
c (Å)	6.1509(7)
α (°)	90
β (°)	90
γ (°)	90
$V(\text{Å}^3)$	541.62(10)
Z	2
ρ_{calc} (g/cm ³)	4.432
M (mm ⁻¹)	20.178
$F(000)$	648.0
Crystal size/mm ³	$0.15 \times 0.12 \times 0.03$
Radiation	Mo K_{α} ($\lambda = 0.71073$ Å)
2θ range for data collection/°	6.14 to 66.56
Index ranges	$-14 \leq h \leq 14, -14 \leq k \leq 14, -9 \leq l \leq 9$
Reflections collected	13569
Independent reflections	1127 [$R_{\text{int}} = 0.0696, R_{\text{sigma}} = 0.0301$]
Data/restraints/parameters	1127/0/36
GoF on F^2	1.104
Final R indexes [$I \geq 2\sigma(I)$]	$R_1 = 0.0219, wR_2 = 0.0501$
Final R indexes [all data]	$R_1 = 0.0228, wR_2 = 0.0505$
Largest diff.peak/hole/e Å ⁻³	2.07/−1.11
Flack parameter	0.12(3)

$$^a R_1 = \Sigma ||F_o| - |F_c|| / \Sigma |F_o|, wR_2 = [\Sigma w(F_o^2 - F_c^2)^2 / \Sigma wF_o^4]^{1/2} \text{ for } F_o^2 > 2\sigma(F_o^2).$$

Table S2. Wyckoff site, fractional atomic coordinates ($\times 10^4$), equivalent isotropic displacement parameters U_{eq} ($\text{\AA}^2 \times 10^3$), and BVS for $\text{Eu}_2\text{ZnGe}_2\text{OS}_6$.

Atom	Wyckoff site	x	y	z	U_{eq}^a	BVS ^b
Eu1	4e	8421.9(2)	6578.1(2)	10020.2(6)	9.34(11)	2.101
Ge1	4e	8729.0(5)	3729.0(5)	5792.8(11)	5.61(16)	4.071
Zn1	2b	5000	5000	5000	8.9(2)	2.122
S1	8f	6758.9(13)	4371.5(14)	7482(2)	8.6(2)	-2.156
S2	4e	8651.5(14)	3651.5(14)	2311(3)	9.8(3)	-1.968
O1	2c	10000	5000	6976(12)	11.7(15)	-1.907

^a U_{eq} is defined as one-third of the trace of the orthogonalized U_{ij} tensor.

^bThe bond valence sums (BVS) of $\text{Eu}_2\text{ZnGe}_2\text{OS}_6$ were calculated by bond-valence parameters method through the following empirical expression¹:

$$\sum_j v_{ij} = V_i$$

$$v_{ij} = \exp[(R_{ij} - d_{ij})/b]$$

Where v_{ij} is the valence of a bond between two atoms i and j, V_i is the sum of all the valences from a given

atom i, R_{ij} is the bond valence parameter, d_{ij} is actual length and b is commonly taken to be a universal

constant equal to 0.37 \AA .

Table S3. Selected bond lengths (Å) and bond angles (°) for Eu₂ZnGe₂OS₆.

Atom–Atom	Length(Å)	Atom–Atom	Length(Å)
Eu–S1	3.0265(14)	Ge1–S1	2.2048(13)
Eu–S1 ^{#2}	3.0429(13)	Ge1–S1 ^{#8}	2.2048(13)
Eu–S1 ^{#3}	3.0429(13)	Ge1–S2	2.1442(18)
Eu–S1 ^{#4}	3.0265(14)	Ge1–O	1.837(3)
Eu–S2 ^{#5}	3.0941(14)	Zn–S1	2.3245(13)
Eu–S2 ^{#6}	3.1027(18)	Zn–S1 ^{#6}	2.3245(13)
Eu–S2 ^{#7}	3.0941(14)	Zn–S1 ^{#9}	2.3245(13)
Eu–O	2.809(5)	Zn–S1 ^{#10}	2.3245(13)
Atom–Atom–Atom	Angle (°)	Atom–Atom–Atom	Angle (°)
S1–Ge–S1 ^{#8}	103.67(7)	S1 ^{#9} –Zn–S1 ^{#5}	97.88(6)
S2–Ge–S1 ^{#8}	116.85(5)	S1 ^{#5} –Zn–S1	115.56(3)
S2–Ge–S1	116.85(5)	S1 ^{#5} –Zn–S1 ^{#10}	115.56(3)
O–Ge–S1	100.38(14)	S1 ^{#10} –Zn–S1	97.88(6)
O–Ge–S1 ^{#8}	100.38(14)	S1 ^{#9} –Zn–S1	115.56(3)
O–Ge–S2	116.1(2)	S1 ^{#9} –Zn–S1 ^{#10}	115.56(3)

Symmetry transformations used to generate equivalent atoms:

#1: 2-X, 1-Y, +Z; #2: 1.5-X, 0.5+Y, 2-Z; #3: 1.5-Y, 1.5-X, +Z; #4: 1-Y, +X, 2-Z;
 #5: 1-Y, +X, 1-Z; #6: 2-X, 1-Y, 1+Z; #7: +X, +Y, 1+Z; #8: 0.5+Y, -0.5+X, +Z;
 #9: +Y, 1-X, 1-Z; #10: 1-X, 1-Y, +Z; #11: +Y, 1-X, 2-Z; #12: +X, +Y, -1+Z;
 #13: 2-X, 1-Y, -1+Z;

Table S4. The dipole moment direction and magnitude (in Debye) of $[\text{ZnS}_4]^{6-}$ and $[\text{GeOS}_3]^{4-}$ units in $\text{Eu}_2\text{ZnGe}_2\text{OS}_6$.

Compound	Unit	a	b	c	Magnitude
$\text{Eu}_2\text{ZnGe}_2\text{OS}_6$	$[\text{ZnS}_4]^{6-}$	0	0	-0.002	0.002
	$[\text{GeOS}_3]^{4-}$	-13.908	-13.908	-6.784	20.806

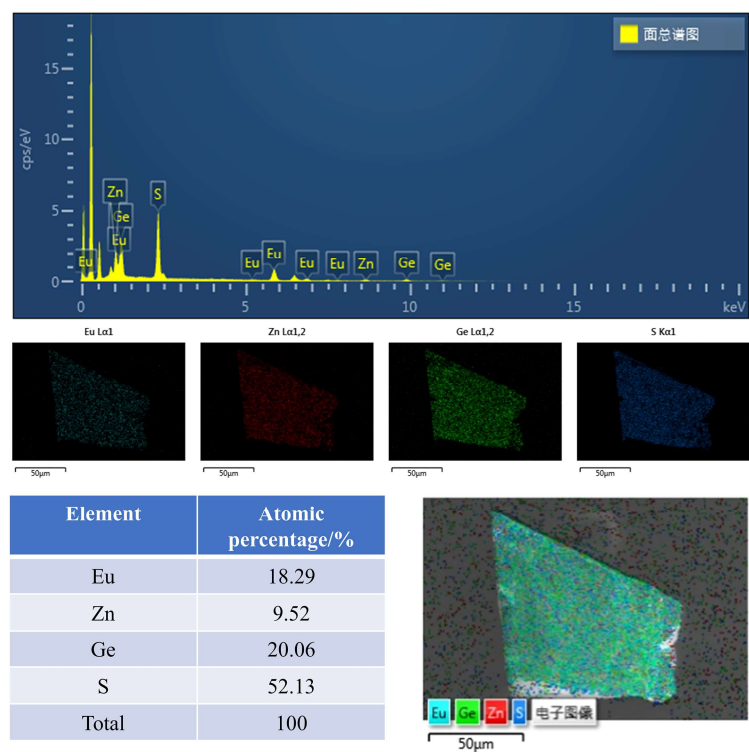


Figure S1. The element distribution images and atomic percentage (%) of $\text{Eu}_2\text{ZnGe}_2\text{OS}_6$.

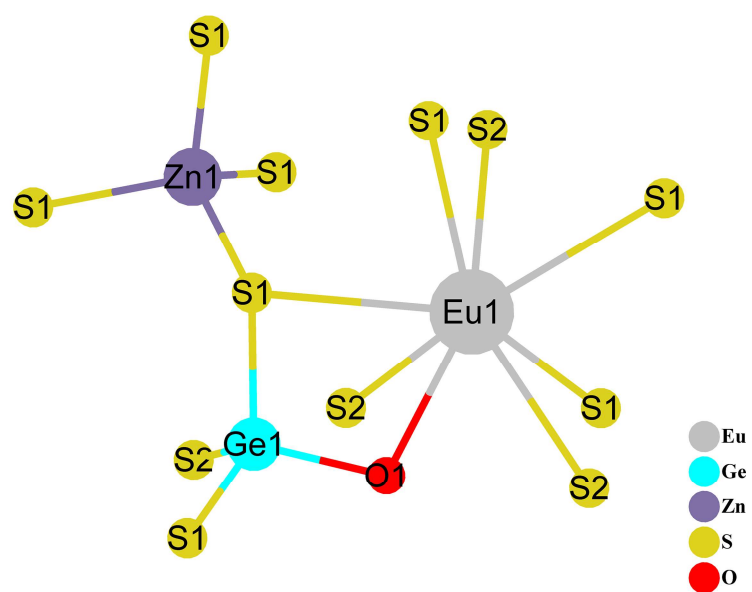


Figure S2. The coordination geometry of $\text{Eu}_2\text{ZnGe}_2\text{OS}_6$.

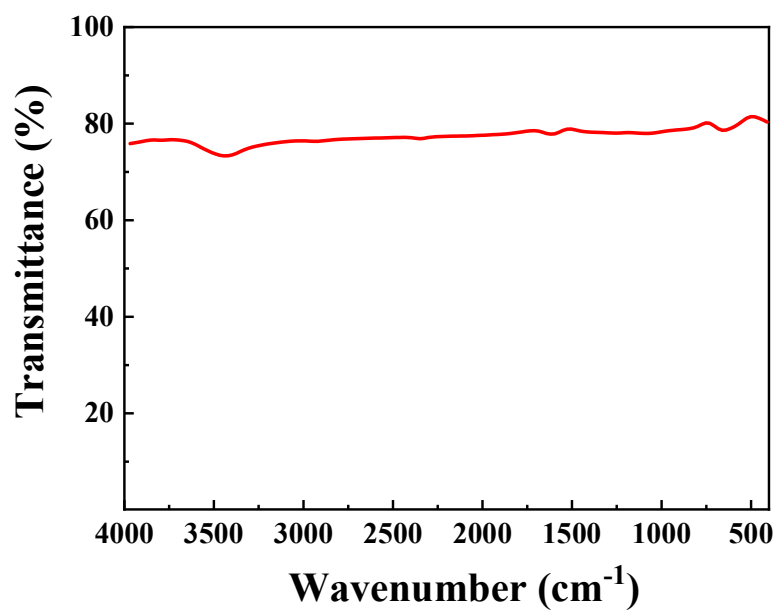


Figure S3. The IR spectrum of $\text{Eu}_2\text{ZnGe}_2\text{OS}_6$.

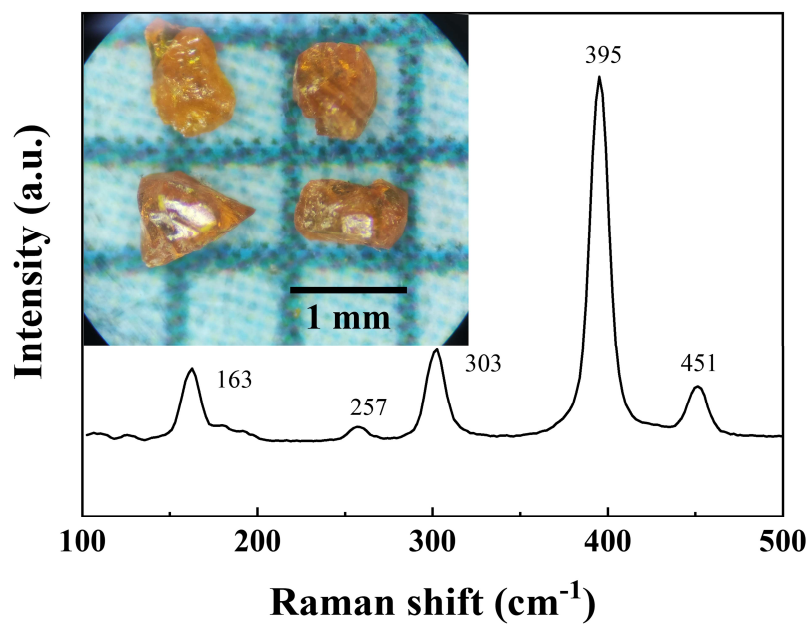


Figure S4. The Raman spectrum of $\text{Eu}_2\text{ZnGe}_2\text{OS}_6$ (inset: $\text{Eu}_2\text{ZnGe}_2\text{OS}_6$ single crystals).

References

- (1) Sheldrick, G. Crystal structure refinement with SHELXL. *Acta Crystallogr., Sect. C: Struct. Chem.* **2015**, *71*, 3-8.
- (2) Macrae, C. F.; Sovago, I.; Cottrell, S. J.; Galek, P. T. A.; McCabe, P.; Pidcock, E.; Platings, M.; Shields, G. P.; Stevens, J. S.; Towler, M.; Wood, P. A. Mercury 4.0: from visualization to analysis, design and prediction. *J. Appl. Crystallogr.* **2020**, *53*, 226-235.
- (3) Simmons, E. L. Diffuse reflectance spectroscopy: a comparison of the theories. *Appl. Opt.* **1975**, *14*, 1380-1386.
- (4) Clark, S. J.; Segall, M. D.; Pickard, C. J.; Hasnip, P. J.; Probert, M. J.; Refson, K.; Payne, M. C. First principles methods using CASTEP. *Zeitschrift Fur Kristallographie* **2005**, *220*, 567-570.
- (5) Ceperley, D. M.; Alder, B. J. Ground State of the Electron Gas by a Stochastic Method. *Phys. Rev. Lett.* **1980**, *45*, 566-569.
- (6) Dal Corso, A.; Pasquarello, A.; Baldereschi, A. Density-functional perturbation theory for lattice dynamics with ultrasoft pseudopotentials. *Phys. Rev. B* **1997**, *56*, R11369-R11372.
- (7) Godby, R. W.; Schlüter, M.; Sham, L. J. Self-energy operators and exchange-correlation potentials in semiconductors. *Phys. Rev. B* **1988**, *37*, 10159-10175.